

Single-crystal elasticity of zoisite $\text{Ca}_2\text{Al}_3\text{Si}_3\text{O}_{12}(\text{OH})$ by Brillouin scattering

ZHU MAO,* FUMING JIANG, AND THOMAS S. DUFFY

Department of Geosciences, Princeton University, Princeton, New Jersey 08544, U.S.A

ABSTRACT

The single-crystal elastic constants of zoisite $\text{Ca}_2\text{Al}_3\text{Si}_3\text{O}_{12}(\text{OH})$ were determined by Brillouin scattering at ambient conditions. The elastic tensor was obtained by an inversion of acoustic velocity data for three different crystal planes. The aggregate bulk modulus, shear modulus, and Poisson's ratio are $K_{\text{S0}} = 125.3(4)$ GPa, $G_0 = 72.9(2)$ GPa, and $\sigma_0 = 0.26(1)$ for the VRH (Voigt-Reuss-Hill) average, respectively. The maximum azimuthal anisotropy of zoisite is 22% for compressional velocity and 33% for shear velocity. The maximum shear splitting is 21% along the [001] direction. Our results resolve the discrepancies in bulk modulus and axial compressibilities reported from static compression studies, and provide the first experimental constraints on the shear modulus. Trends in the elastic moduli of minerals in the CaO-Al₂O₃-SiO₂-H₂O (CASH) system are evaluated.

Keywords: Zoisite, single crystal, elasticity, Brillouin scattering

INTRODUCTION

Hydrous phases in subduction zones are potential agents that can transport water to the deep earth. Properties of these hydrous minerals, especially elastic moduli, are necessary to model seismic wave speeds and hence place constraints on recycling of H₂O through subduction zones (Hacker et al. 2003). Zoisite $\text{Ca}_2\text{Al}_3\text{Si}_3\text{O}_{12}(\text{OH})$ is a hydrous mineral containing 2 wt% water that is potentially important in subduction zones. It has a large stability field that extends up to 5.0 GPa at 700 °C and 6.6 GPa at 950 °C in the CaO-Al₂O₃-SiO₂-H₂O (CASH) system (Poli and Schmidt 1998). In the basalt + H₂O system, zoisite remains stable to pressures of 3.1 GPa at 650 °C (Fornieris and Holloway 2003). Breakdown of zoisite at this pressure may be a source of fluid release at 100–120 km depth depending on the thermal structure of the subducting slab (Poli and Schmidt 1995).

Zoisite belongs to epidote group $[\text{Ca}_2(\text{Al,Fe})_3\text{Si}_3\text{O}_{12}(\text{OH})]$, which occur in high- and ultrahigh-pressure metamorphic rocks from a wide variety of geological settings, including continental collisions and subduction zones (Hacker et al. 2003; Enami et al. 2004). Figure 1 shows the crystal structure of zoisite (Fesenko et al. 1955; Fesenko et al. 1956; Dollase 1968). Zoisite is the only member of the epidote group that is orthorhombic, instead of monoclinic. However, the structures of all epidote minerals are similar. Monoclinic epidotes, including clinozoisite, have two distinct edge sharing octahedral chains that run along [010]. The octahedral sites are mainly occupied by Al but can also contain Fe³⁺. Zoisite has only one type of octahedral chain parallel to [010] made up of edge sharing octahedra designated M1,2. The second octahedral site, M3, is more distorted and is attached to M1,2 by edge sharing. The parallel octahedral chains are linked by SiO₄ and Si₂O₇ tetrahedral groups for both types of epidote minerals. Calcium ions reside in two large positions between

the octahedral chains and exhibit sevenfold coordination. Hydrogen is bonded to an oxygen in the octahedral chains (Franz and Liebscher 2004).

Zoisite is structurally related to some other Ca-Al silicates that may also be important in subduction zones, including lawsonite $\text{CaAl}_2\text{Si}_2\text{O}_7(\text{OH})_2 \cdot (\text{H}_2\text{O})$ and pumpellyite $\text{Ca}_2\text{MgAl}_2(\text{SiO}_4)(\text{SiO}_7)(\text{OH})_2 \cdot (\text{H}_2\text{O})$. The lawsonite structure, for example, also consists of chains of edge-sharing AlO₆ octahedra but linked by Si₂O₇ groups only. The large cavities are occupied by Ca atoms and H₂O molecules.

Only a limited amount of Fe³⁺-Al substitution is observed in zoisite and so it is chemically more restricted to compositions close to end-member $\text{Ca}_2\text{Al}_3\text{Si}_3\text{O}_{12}(\text{OH})$ compared with the monoclinic epidotes. The highest Fe³⁺ content found in zoisite is $X_{\text{Fe}} = 0.21\text{--}0.23$ (Vogel and Bahezre 1965; Brunsmann et al. 2000).

Knowing the bulk modulus of zoisite is necessary to calculate seismic wave velocities and for volume determination at high pressures in phase equilibria calculations. The bulk modulus has been determined from static pressure-volume measurements using X-ray diffraction in both multi-anvil apparatus and diamond anvil cells (Holland et al. 1996; Comodi and Zanazzi 1997; Pawley et al. 1998; Grevel et al. 2000). Existing results show large discrepancies. The zero-pressure isothermal bulk modulus K_{T0} ranges from 102(6.5) GPa (Comodi and Zanazzi 1997) to 279(9) GPa (Holland et al. 1996). Neglecting the anomalous result of Holland et al. (1996), the range of possible bulk moduli for zoisite translate into a 3% uncertainty in the bulk sound velocity at 6 GPa (Hacker et al. 2003). Even more importantly, the shear and compressional sound velocities are unknown because of lack of constraint on the shear modulus. For the monoclinic epidotes, a large range of bulk moduli have also been reported from previous experiments ranging from 106.2 to 207 GPa (Ryzhova et al. 1966; Holland et al. 1996; Qin et al. 2003).

In this study, we used Brillouin scattering and X-ray diffraction to determine the full elastic tensor of zoisite. In doing so, we

* E-mail: zhuma@princeton.edu

could resolve discrepancies in the bulk modulus and determine the shear modulus and elastic anisotropy for the first time. Zoisite is a good choice for initial studies of the elasticity of epidote minerals because of its higher symmetry and limited range of chemical variability (Franz and Liebscher 2004). We also compared the elasticity of zoisite to that of other minerals in the CASH system.

EXPERIMENTS

Three platelets were cut from a gem-quality zoisite sample of unknown origin. Energy-dispersive single-crystal X-ray diffraction was performed at beamline X17C of the National Synchrotron Light Source. The unit-cell parameters were determined to be $a = 16.207(5)$, $b = 5.540(5)$, and $c = 10.056(2)$ Å with a calculated density $3.343(3)$ g/cm³ in good agreement with literature values (Franz and Liebscher 2004). The chemical composition was measured by electron microprobe and showed the sample to be pure zoisite with Fe, Mn, and Mg below detection limits. Figure 2 shows the Raman spectra of zoisite under ambient conditions. 29 modes were observed in this study and are compared with previous work (Huang 1999) in Table 1. Peak positions are generally in good agreement with Huang (1999) but we are able to identify several additional modes. The symmetric OH stretching vibration is observed at 3150.2 cm⁻¹.

All three platelets were carefully polished parallel on both sides to 0.5 mm thickness using alumina paper down to a grit size of 1 μm. The Brillouin spectra were measured using a six-pass Sandercock tandem Fabry-Perot interferometer in a forward symmetric scattering geometry under ambient conditions. The sample was excited by a solid-state laser with a wavelength of 532.15 nm and power of about 150 mW. The acoustic velocities, v , are determined from the measured Brillouin frequency shift $\Delta\nu_B$:

$$v = \frac{\Delta\nu_B \lambda_0}{2 \sin(\theta/2)} \quad (1)$$

where λ_0 is the incident wavelength, θ is the scattering angle (70° in this study). Details of the Brillouin system are given elsewhere (Speziale and Duffy 2002).

Measurements were made in a total of 37 directions at 5° steps for each platelet. For each spectrum, the average collection time was around 20 minutes. Our Brillouin spectra are of excellent quality with a high signal-to-noise ratio. One quasi-longitudinal and two quasi-transverse waves were observed in most directions for all three platelets (Fig. 3). The uncertainty of the measurement was within $\pm 0.5\%$ of the measured velocities.

RESULTS

Zoisite has orthorhombic symmetry (space group $Pnma$) and nine independent elastic constants. For each platelet, the direction cosine that describes the phonon propagation direction can be described by an azimuthal angle together with the three Eulerian

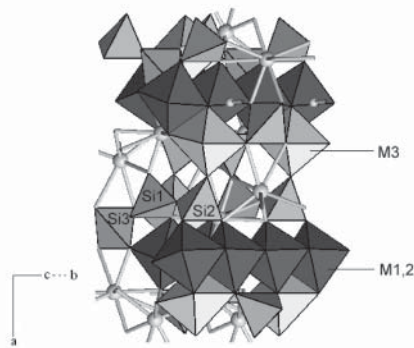


FIGURE 1. The crystal structure of zoisite. Zoisite is characterized by a single octahedron chain with site M1,2. M3 octahedra are attached to M1,2 by edge sharing. There are three distinct Si sites. Si1 and Si2 form a Si_2O_7 group. Si3 is an isolated tetrahedron. The large spheres represent Ca atoms. The small spheres are hydrogen sites.

angles that relate the laboratory and crystal coordinate systems (Shimizu 1995). In fitting all the velocity data for the three platelets together, there are thus a total of 18 parameters (nine elastic constants, nine Eulerian angles) to be constrained. These

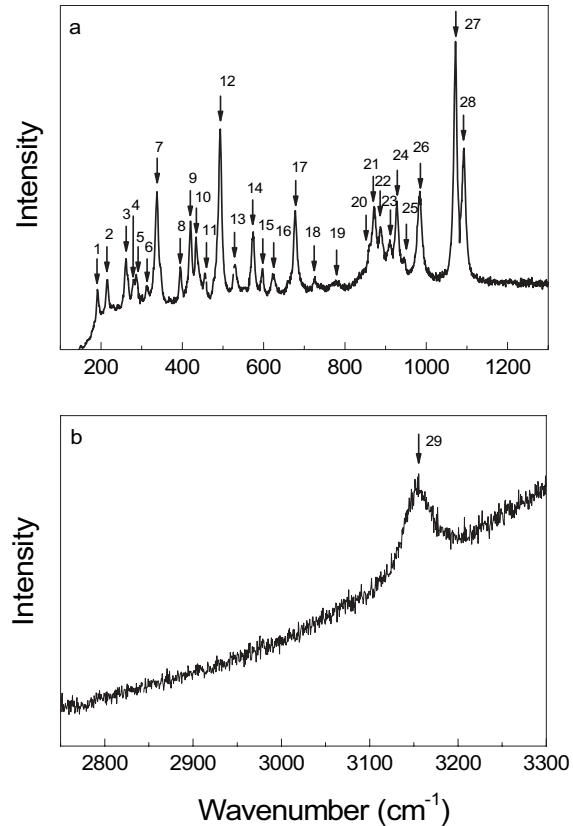


FIGURE 2. Raman spectra of zoisite under ambient conditions. (a) Wavenumber ranges from 100 to 1300 cm⁻¹; (b) Raman spectrum of OH stretching vibration.

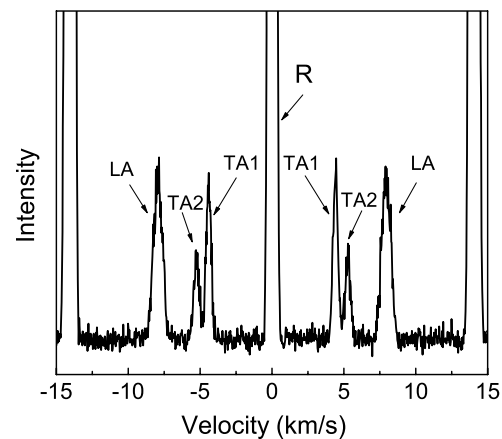


FIGURE 3. Brillouin spectrum of zoisite at ambient conditions (sample 1, azimuthal angle = 30°). R = unshifted Rayleigh line; LA = longitudinal mode; TA1, TA2 = two transverse modes. TA2 is the fast transverse mode.

TABLE 1. Peak positions in Raman spectrum of zoisite

| No. | This study (cm ⁻¹) | Huang 1999 (cm ⁻¹) | No. | This study (cm ⁻¹) | Huang 1999 (cm ⁻¹) | No. | This study (cm ⁻¹) | Huang 1999 (cm ⁻¹) | No. | This study (cm ⁻¹) | Huang 1999 (cm ⁻¹) |
|-----|-----------------------------------|-----------------------------------|-----|-----------------------------------|-----------------------------------|-----|-----------------------------------|-----------------------------------|-----|-----------------------------------|-----------------------------------|
| 1 | 191.7 | 186 | 2 | 215.2 | 217 | 3 | 261.4 | 257 | 4 | 280.2 | 269 |
| 5 | 287.1 | | 6 | 312.1 | 310 | 7 | 337.4 | 338 | 8 | 395.3 | 396 |
| 9 | 419.8 | | 10 | 434.8 | 431 | 11 | 455.6 | | 12 | 492.9 | 490 |
| 13 | 529.6 | 528 | 14 | 573.7 | 572 | 15 | 597.1 | 594 | 16 | 623.3 | 620 |
| 17 | 677.8 | 678 | 18 | 727.0 | | 19 | 777.5 | | 20 | 860.3 | |
| 21 | 871.7 | 869 | 22 | 889.0 | | 23 | 909.0 | | 24 | 927.8 | 926 |
| 25 | 945.8 | | 26 | 983.4 | 982 | 27 | 1017.7 | 1070 | 28 | 1092.3 | 1091 |
| 29 | 3150.2 | 3151 | | | | | | | | | |

were obtained by non-linear least squares fitting to Christoffel's equation (Every 1980):

$$\det|C_{ijkl}n_jn_l - \rho v^2\delta_{ik}| = 0 \quad (2)$$

where, ρ is the density, v is the velocity of phonon, n_i are the direction cosines of the phonon propagation directions, and the C_{ijkl} are the elastic constants. Table 2 shows the best-fitting C_{ij} values. Here we have adopted the compact Voigt notation for the components of the elastic tensor (Nye 1985). Orientations of two of the three crystal platelets were determined by energy-dispersive single-crystal X-ray diffraction at beamline X17C of Brookhaven National Laboratory (Hu et al. 1994). The X-ray orientations were used as starting models in the inversion. Table 3 shows the Eulerian angles obtained from inversion of the Brillouin scattering data compared with those from single-crystal X-ray diffraction. The uncertainty on Eulerian angles that results from the inversion is typically within 1.5°. The single-crystal X-ray orientations are similar, but can show differences from Brillouin results up to 5°. The difference is likely to due to the remounting of the crystal that was necessary for the X-ray measurements but tradeoffs among the Eulerian angles for a given plane may also contribute as discussed below.

Figure 4 shows the experimentally obtained velocity data together with values calculated from the best fitting elastic constants. The root-mean-square (RMS) deviation between measured and calculated acoustic velocities was 39 m/s. For the longitudinal moduli C_{11} , C_{22} , C_{33} and shear moduli C_{44} , C_{55} , C_{66} , the precision of the recovered value is better than 0.6% (1 σ level), while it is better than 2.6% for the off-diagonal moduli C_{12} , C_{13} , C_{23} . The covariance matrix was calculated and indicates that individual constants are well resolved and do not suffer significant "trade-offs" among pairs of elastic constants (Press et al. 1988; Brown et al. 1989). The greatest trade-offs are between C_{12} and C_{13} and between C_{23} and C_{13} , but the magnitude of the covariance coefficients are less than 2% of the magnitude of the constants themselves.

DISCUSSION

Individual moduli and elastic anisotropy of zoisite

The individual elastic moduli of zoisite can be compared to values for other hydrous Ca-Al silicates such as lawsonite (Sinogeikin et al. 2000) and hibschtite (O'Neill et al. 1993) (Table 4). In general, the longitudinal, shear, and off-diagonal moduli of zoisite span similar ranges as those observed for the other materials, but the maximum values for each type of modulus in zoisite exceeds those in the other minerals. The longitudinal modulus along the direction of the octahedral chains is interme-

TABLE 2. Single-crystal elastic moduli of zoisite

| Modulus | Value (GPa) | Modulus | Value (GPa) | Modulus | Value (GPa) |
|----------|-------------|----------|-------------|----------|-------------|
| C_{11} | 279.8(6) | C_{44} | 51.8(3) | C_{12} | 94.7(11) |
| C_{22} | 249.2(6) | C_{55} | 81.4(3) | C_{13} | 88.7(10) |
| C_{33} | 209.4(9) | C_{66} | 66.3(3) | C_{23} | 27.5(7) |

Note: Numbers in parentheses are 1- σ uncertainty in the last digit(s).

TABLE 3. Eulerian angles from single crystal X-ray diffraction and Brillouin scattering

| Experimental technique | Sample 2 | | Sample 3 | |
|---------------------------|-----------|-----------|-----------|---------|
| | θ | χ | θ | χ |
| X-ray | 56.3° | 94.8° | 106.3° | 6.8° |
| Brillouin | 51.8(14)° | 97.3(13)° | 106.3(7)° | 5.7(6)° |

TABLE 4. Single-crystal elastic moduli of zoisite, lawsonite, and hibschtite

| Modulus | Zoisite | Lawsonite* | Hibschtite† |
|----------------|----------|------------|-------------|
| C_{11} (GPa) | 279.8(6) | 226(2) | 186.5(11) |
| C_{22} (GPa) | 249.2(6) | 214(2) | 186.5(11) |
| C_{33} (GPa) | 209.4(9) | 259(2) | 186.5(11) |
| C_{44} (GPa) | 51.8(3) | 65(1) | 63.9(5) |
| C_{55} (GPa) | 81.4(3) | 60(1) | 63.9(5) |
| C_{66} (GPa) | 66.3(3) | 17(1) | 63.9(5) |
| C_{12} (GPa) | 94.7(11) | 69(2) | 56.5(14) |
| C_{13} (GPa) | 88.7(10) | 65(2) | 56.5(14) |
| C_{23} (GPa) | 27.5(7) | 82(2) | 56.5(14) |

* From Sinogeikin et al. (2000).

† From O'Neill et al. (1993). The composition is Ca₂Al₂(SiO₄)_{1.72}(H₂O₄)_{1.28}.

diate in value for zoisite, which is also the case for lawsonite. Among the shear moduli, C_{55} for zoisite is 23% larger than C_{44} and 55% larger than C_{66} . One exceptional feature of the elasticity of zoisite is that C_{23} is much lower than C_{12} and C_{23} or any of the off-diagonal moduli for lawsonite and hibschtite. Data inversions in which C_{23} was fixed at higher values gave poor fits to the velocity data.

The maximum shear velocity for zoisite is 5.47 km/s along [011] (polarization [0, 0.62, -0.79]). The minimum shear velocity is 3.94 km/s along [001] (polarization [010]). [001] is the direction of the maximum shear splitting [($v_{S,max[001]} - v_{S,min[001]}$)/ $v_{S,aggr}$ = 0.21]. Zoisite has much smaller shear anisotropy $A_S = [(v_{S,max} - v_{S,min})/v_{S,aggr} = 0.33]$ than lawsonite at ambient P and T ($A_S = 0.74$) (Sinogeikin et al. 2000). However, lawsonite exhibits strong shear softening at ambient T as discussed below and its anisotropy is much reduced upon heating to 450 °C ($A_S = 0.40$) (Schilling et al. 2003). The longitudinal anisotropy of zoisite $A_P = [(v_{P,max} - v_{P,min})/v_{P,aggr} = 0.22]$ is smaller than the shear anisotropy. It is comparable to that of lawsonite ($A_P = 0.24$) (Sinogeikin et al. 2000).

Aggregate elasticity and comparison with previous studies

Table 5 presents the Voigt and Reuss bounds and VRH average (Voigt-Reuss-Hill) for the isotropic aggregate bulk and shear modu-

lus. The aggregate Poisson's ratio is 0.26(1), which is given by

$$\sigma = \frac{3K - 2G}{2(3K + G)} \quad (3)$$

where K is the bulk modulus, G is the shear modulus.

The isothermal bulk modulus, K_T , was calculated from the measured adiabatic value, K_S , using

$$K_T = K_S / (1 + \alpha\gamma T) \quad (4)$$

where T is temperature (300 K), α is the thermal expansion coefficient, and γ is the Gruneisen parameter given by

$$\gamma = \frac{\alpha K_S V}{C_P} \quad (5)$$

V is the molar volume and C_P is the specific heat. Thermodynamic values used for the adiabatic to isothermal correction are

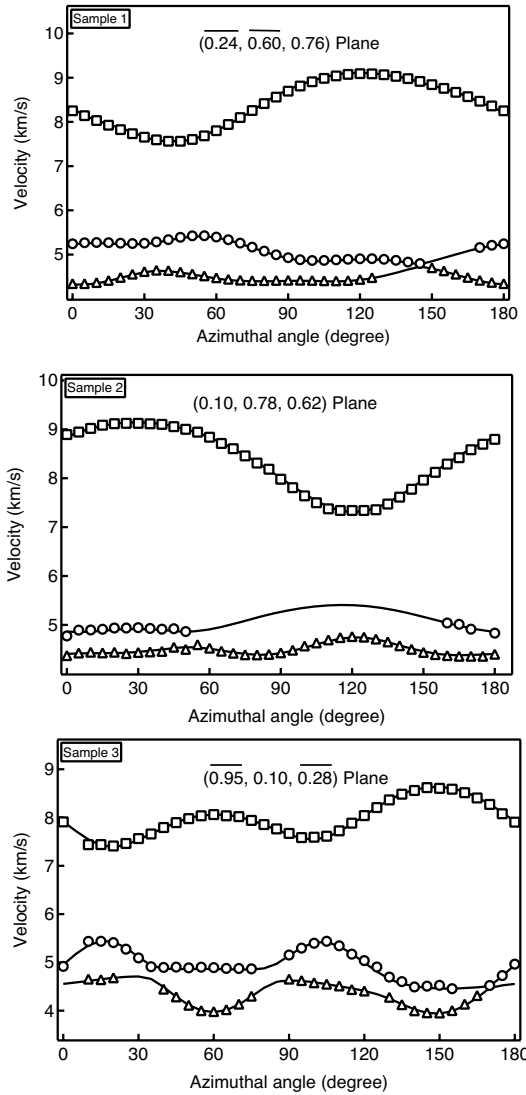


FIGURE 4. Measured compressional and shear wave speeds of zoisite as a function of direction for three platelets of zoisite. Symbols represent experimental velocities. Solid lines are best fitting results.

shown in Table 6.

Our resulting $K_{T0} = 123.4(4)$ GPa is in agreement with those of Pawley et al. (1998) and Grevel et al. (2000) who used the Birch-Murnaghan equation of state to fit pressure-volume data (Table 7). Our result is also within 5% of that reported from first principles calculations using density functional theory ($K_{T0} = 117.5$ GPa) (Winkler et al. 2001a). On the other hand, our value is 17% higher than $K_{T0} = 102.6$ GPa reported by Comodi and Zanazzi (1997). The determination of the bulk modulus and its pressure derivative in static compression studies relies on the fits to the slope of the measured P - V curve. Static compression studies also suffer from a well-known tradeoff between fitted values of the pressure derivative of the bulk modulus, K'_{T0} , and K_{T0} . The limited pressure ranges in previous compression studies could lead to large uncertainties in the bulk modulus.

Using V_0 , K_{T0} values from our X-ray and Brillouin data, we calculated the pressure volume isotherm using the third-order Birch-Murnaghan equation of state by assuming $K'_{T0} = 4$ (Fig. 5). In general, our compression curve is broadly consistent with earlier measurements and the agreement is especially good for the equation of state of Grevel et al. (2000).

Previous theoretical and experimental studies that examined both zoisite and clinozoisite found that the bulk modulus of clinozoisite is 20% greater than that of zoisite (Comodi and Zanazzi 1997; Winkler et al. 2001a). However, in the experi-

TABLE 5. Aggregate elastic moduli of zoisite

| This study | Reuss | Voigt | VRH |
|----------------|----------|----------|----------|
| K_{S0} (GPa) | 121.6(4) | 128.9(4) | 125.3(3) |
| G_0 (GPa) | 70.6(2) | 75.1(2) | 72.9 (2) |
| v_p (km/s) | 8.03 | 8.28 | 8.16 |
| v_s (km/s) | 4.60 | 4.74 | 4.67 |
| σ_0 | 0.26(1) | 0.26(1) | 0.26(1) |

TABLE 6. Thermodynamic parameters of zoisite under ambient conditions

| Parameter | Value | Reference |
|-------------------------------|--------------------------------------|---|
| Thermal expansion, α | $3.29 \times 10^{-5} \text{ K}^{-1}$ | Pawley et al. (1998); Grevel et al. (2000) |
| Molar volume, V | 135.9(2) cm^3 | This study |
| Gruneisen parameter, γ | 1.59 | Calculated |
| Heat capacity, C_p | 352 J/(K-mol) | Poli and Schmidt (1998) |

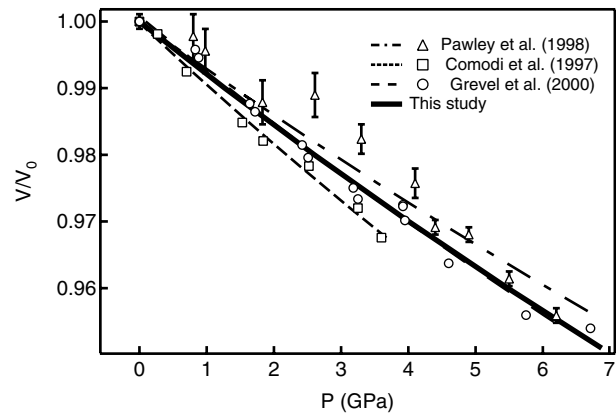


FIGURE 5. Volume compression of zoisite as a function of pressure at room temperature from Brillouin scattering (thick solid line) and static compression experiments. Error bars are smaller than symbols when not shown.

TABLE 7. Isothermal bulk modulus and shear modulus of zoisite and related minerals

| Mineral | Reference | P_{max} (GPa) | K_{T0} (GPa) | K_T (GPa) | K'_{T0} * | G_0 (GPa) |
|-------------|---------------------------|-----------------|----------------|-------------|-------------|-------------|
| Zoisite | This study | 0 | 125.3(3) | 123.4(4) | | 72.9(2) |
| | Pawley et al. (1998) | 6.2 | | 125(3) | 4 (fixed) | |
| | Grevel et al. (2000) | 7 | | 125.1(2.1) | 4 (fixed) | |
| | Comodi and Zanazzi (1997) | 3.6 | | 102(6.5) | 4.8(4) | |
| Clinzoisite | Winkler et al. (2001b) | 0 | | 117.5(1.7) | | |
| | Comodi and Zanazzi (1997) | 5.1 | | 127.0(4.5) | 0.5(2) | |
| | Winkler et al. (2001a) | 0 | | 136(4) | | |
| Epidote | Holland et al. (1996) | 5.21 | | 162(4) | 4 (fixed) | |
| | Ryzhova (1966) | 0 | 106.2 | | | 61.2 |
| | Qin et al. (2003) | 20 | | 207(15) | 4 (fixed) | |
| Lawsonite | Sinogeikin et al. (2000) | 0 | 125(2) | 123.2(20) | | 51.8(7) |

* $K'_{T0} = (\partial K_{T0} / \partial P)_T$

mental static compression study of Comodi and Zanazzi (1997), fits were performed using $K'_{T0} = 0.5$ for clinzoisite and $K'_{T0} = 4.8$ for zoisite. If a value of $K'_{T0} = 4$ were adopted for the former and the equation of states refitted, K_T would decrease to 117 GPa, which is now smaller than that of zoisite. Thus, at present there are no experimental results that can unambiguously confirm the theoretical finding that there is a significant difference between the bulk moduli of zoisite and clinzoisite.

For orthorhombic crystals, the linear compressibilities along the three crystallographic axes are given by Nye (1985):

$$\begin{aligned}\beta_a &= s_{11} + s_{12} + s_{13} \\ \beta_b &= s_{21} + s_{22} + s_{23} \\ \beta_c &= s_{31} + s_{32} + s_{33}\end{aligned}\quad (6)$$

where β_i is the linear compressibility in the i direction, and s_{ij} are the isothermal elastic compliances. The conversion of adiabatic elastic constants to isothermal ones (Davies 1974) was carried out using parameters in Table 2. From our measured elastic constants, the values calculated for zoisite at ambient conditions are:

$$\begin{aligned}\beta_a &= 1.36(3) \times 10^{-3} \text{ GPa}^{-1} \\ \beta_b &= 3.13(2) \times 10^{-3} \text{ GPa}^{-1} \\ \beta_c &= 3.85(2) \times 10^{-3} \text{ GPa}^{-1}\end{aligned}\quad (7)$$

Figure 6 shows relative axial compressibilities of zoisite computed using elastic constants in comparison with those determined by static compression studies. In this case, we have not included any pressure effects on the s_{ij} and hence our axial compressibilities are close to straight lines (solid lines in Fig. 6). In reality, the effect of the decreased compressibility with pressure means our measurements give a lower bound to the actual axial compression curves. For the a and b axes, our results are in a general agreement with Grevel et al. (2000). While for the c axis, our result instead agrees best with that of Comodi and Zanazzi (1997). If the pressure effect is considered, this will lead to a better agreement in b and c axes with previous studies but poorer agreement for the a axis.

Elasticity in CaO-Al₂O₃-SiO₂-H₂O system

Figure 7 shows selected minerals in the CASH system. The chemical compositions are listed in Table 8. Minerals in this system can be grouped by similarities in chemical compositions. Some phases are polymorphs: zoisite and clinzoisite;

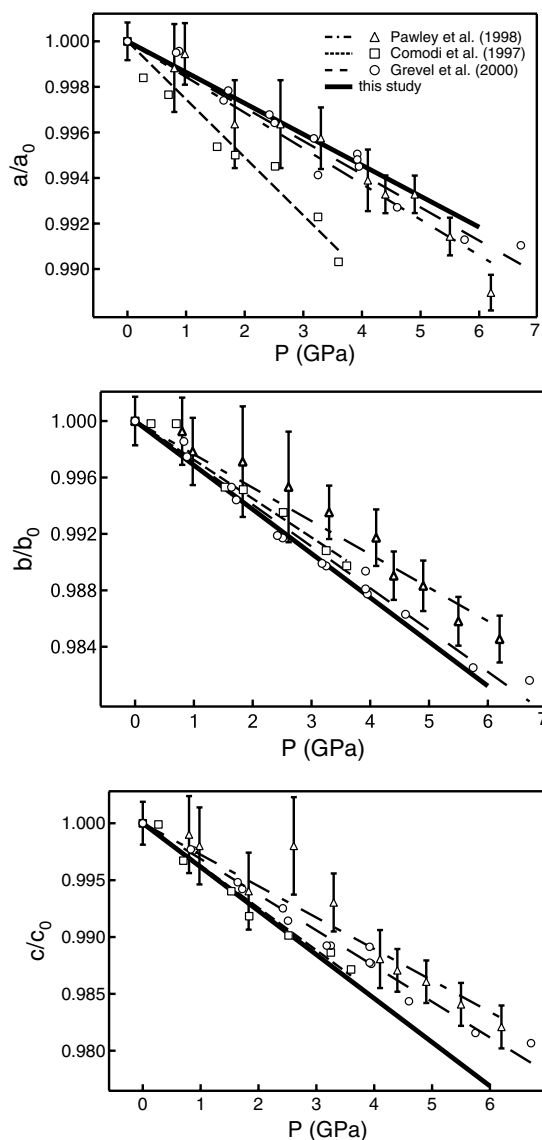


FIGURE 6. Relative compression of unit-cell parameters of zoisite derived from Brillouin scattering data (thick solid line) compared with static compression studies. Error bars are smaller than symbols when not shown.

kyanite, sillimanite, and andalusite; quartz and coesite. Lawsonite, diaspore, and portlandite are chemically hydrous forms of anorthite, corundum, and lime, respectively, but with different crystal structures. Hibschite is the hydrous phase of grossular with which it forms a solid solution. The hydrous Ca-Al silicates: lawsonite and zoisite contain 11.5 and 2 wt% H₂O, respectively. Hibschite has variable H₂O content, but elasticity data have been reported for a sample with composition Ca₃Al₂(SiO₄)_{1.72}(H₄O₄)_{1.28} containing 10.9 wt% H₂O (O'Neill et al. 1993).

Figure 8 shows the bulk and shear moduli of minerals in the CASH system. Although a wide range of structures, compositions, and water contents are represented, both the bulk and shear modulus show a general, monotonic increase of moduli with density. With the exception of anorthite-lawsonite, incorporation of water decreases the density and elastic moduli of minerals in the CASH system: the elastic moduli of diaspore, portlandite, hibschite are smaller than the chemically related anhydrous phases corundum, lime, and grossular. The modulus-density trend for the hydrous-anhydrous pairs tends to follow the general behavior of the CASH system as a whole.

Lawsonite and zoisite have similar structures. Lawsonite consists of chains of edge sharing AlO₆ octahedra in [100] direction and are linked by Si₂O₇ tetrahedra along [001] direction. Water is present as both H₂O molecules and OH groups, and lawsonite contains 11.5 wt% water, which is much greater than that of zoisite (2 wt%). OH groups are bonded to Al-octahedra for both structures. H₂O molecules and Ca atoms occupy large cavities in

the lawsonite structure. At high pressures and temperatures up to 980 °C at 6.5 GPa, lawsonite decomposes into zoisite, kyanite, quartz (coesite), and water (Schmidt and Poli 1994).

The elastic constants of lawsonite have been determined from Brillouin scattering (Sinogeikin et al. 2000; Schilling et al. 2003). Zoisite and lawsonite have very similar bulk moduli, but zoisite has a 40% larger shear modulus than lawsonite (52 GPa). This is likely related to a phase transition in lawsonite at *T* near 0 °C (Sondergeld et al. 2000). Lawsonite exhibits shear softening of the elastic constant *C*₆₆ as the transition temperature is approached. The low shear modulus of lawsonite is strongly affected by the softening of *C*₆₆ (Table 4). As temperature increases, the shear modulus of lawsonite actually increases (Schilling et al. 2003). Due to the proximity of the phase transition in lawsonite at ambient conditions, it is difficult to predict its elasticity at subducting slab conditions.

The density and bulk modulus of lawsonite are greater than its anhydrous counterpart, anorthite, but it has a smaller shear modulus in comparison with anorthite. These features are a reflection of both the elastic instability in lawsonite discussed above as well as the large structural differences between the two minerals. Al in anorthite is in fourfold coordination, but Al in

TABLE 8. Chemical formula of minerals in the CaO-Al₂O₃-SiO₂-H₂O system

| Mineral name | abbr. | Chemical formula | Mineral name | abbr. | Chemical formula |
|--------------|-------|--|--------------|-------|--|
| anorthite | an | CaAl ₂ Si ₂ O ₈ | lawsonite | law | CaAl ₂ Si ₂ O ₇ (OH) ₂ ·H ₂ O |
| grossular | gr | Ca ₃ Al ₂ (SiO ₄) ₃ | hibschite | hib | Ca ₃ Al ₂ (SiO ₄) _{1.72} (H ₄ O ₄) _{1.28} |
| corundum | cor | Al ₂ O ₃ | diaspore | dia | AlOOH |
| lime | lm | CaO | portlandite | prt | Ca(OH) ₂ |
| zoisite | zo | Ca ₂ Al ₃ Si ₃ O ₁₂ (OH) | clinozoisite | czo | Ca ₂ Al ₃ Si ₃ O ₁₂ (OH) |
| quartz | qz | SiO ₂ | coesite | cs | SiO ₂ |
| kyanite | ky | Al ₂ SiO ₅ | sillimanite | sil | Al ₂ SiO ₅ |
| andalusite | and | Al ₂ SiO ₅ | | | |

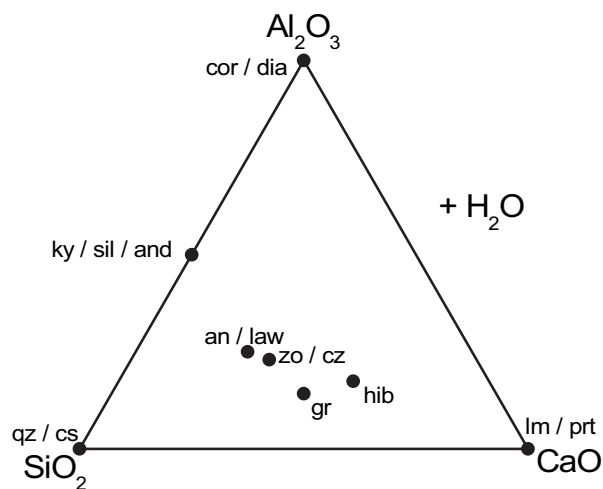


FIGURE 7. Selected minerals in the CaO-Al₂O₃-SiO₂-H₂O system. Chemical compositions and abbreviations are given in Table 8.

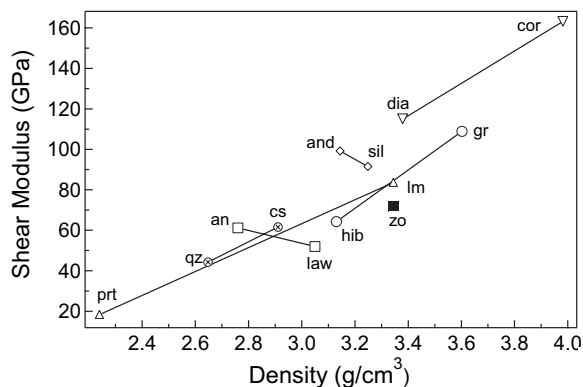
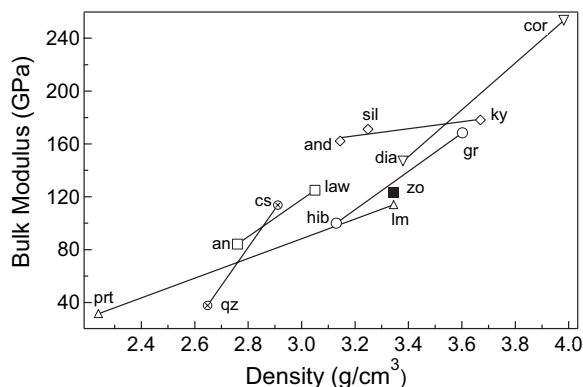


FIGURE 8. Bulk and shear moduli of minerals in the CaO-Al₂O₃-SiO₂-H₂O system. Solid lines connect structurally or chemically related species. Data are from: ky (Winkler et al. 2001b); sil, and (Vaughan and Weidner 1978); an (Hearmon 1984); law (Sinogeikin et al. 2000); cor (Ohno et al. 1986); dia (Jiang et al. 2005); lm (Oda et al. 1992); prt (Laugesen 2005); gr (Bass 1989); hib (O'Neill et al. 1993); qz (Hearmon 1979); cs (Weidner and Carleton 1977). Abbreviations are listed in Table 8.

lawsonite is in sixfold coordination.

In general, Figure 8 shows that structurally and chemically diverse minerals in the CASH system show a general increase in both bulk and shear modulus with density. Structural effects are clearly also important or even dominant as in the case of lawsonite and anorthite. The hydrous Ca-Al silicates (lawsonite, hibschite, zoisite) show an increase in shear modulus with decreasing water content (and increasing density). As discussed above, the shear modulus of lawsonite may be anomalous, and the values for hibschite and zoisite are likely to be more representative of hydrous Ca-Al silicates generally.

ACKNOWLEDGMENTS

We thank J. Hu for assistance with X-ray measurements and Jim Eckert (Yale) for performing the microprobe analysis. We also benefited from discussions with Sergio Speziale. This research was supported by the NSF and the Carnegie-DOE alliance center. Use of the National Synchrotron Light Source, Brookhaven National Laboratory, was supported by the U.S. Department of Energy, Office of Science, Office of Basic Energy Sciences, under contract no. DE-AC02-98CH10886.

REFERENCES CITED

- Bass, J.D. (1989) Elasticity of grossular and spessartine garnets by Brillouin spectroscopy. *Journal of Geophysical Research*, 94, 7621–7628.
- Brown, J.M., Slutsky, L.J., Nelson, K.A., and Cheng, L.T. (1989) Single-crystal elastic constants for San Carlos Peridot: An implication of impulsive stimulated scattering. *Journal of Geophysical Research*, 94, 9485–9492.
- Brunsmann, A., Franz, G., Erzinger, J., and Landwehr, D. (2000) Zoisite- and clinozoisite-segregations in metabasites (Tauern Window, Austria) as evidence for high-pressure fluid-rock interaction. *Journal of Metamorphic Geology*, 18, 1–21.
- Comodi, P. and Zanazzi, P.F. (1997) The pressure behavior of clinozoisite and zoisite: An X-ray diffraction study. *American Mineralogist*, 82, 61–68.
- Davies, D.F. (1974) Effective elastic moduli under hydrostatic stress: I. Quasi-harmonic theory. *Journal of Physics and Chemistry of Solids*, 35, 1513–1520.
- Dollase, W.A. (1968) Refinement and comparison of the structures of zoisite and clinozoisite. *American Mineralogist*, 53, 1882–1898.
- Enami, M., Liou, J.G., and Mattinson, C.G. (2004) Epidote Minerals in High *P/T* Metamorphic Terranes: Subduction Zone and High- to Ultrahigh-Pressure Metamorphism. In A. Liebscher and G. Franz, Eds., *Epidotes*, 56, p. 347–398. *Reviews in Mineralogy and Geochemistry*, Mineralogical Society of America, Chantilly, Virginia.
- Every, A.G. (1980) General closed-form expressions for acoustic waves in elastically anisotropic solids. *Physical Review B*, 22, 1746–1760.
- Fesenko, E.G., Rumanova, I.M., and Belov, N.V. (1955) The crystal structure of zoisite. *Structure Report*, 19, 464–465.
- (1956) Crystal structure of zoisite. *Structure Report*, 20, 396–398.
- Forneris, J.F. and Holloway, J.R. (2003) Phase equilibria in subducting basaltic crust: implications for H₂O release from the slab. *Earth and Planetary Science Letters*, 214, 187–201.
- Franz, G. and Liebscher, A. (2004) Physical and Chemical Properties of the Epidote Minerals—An Introduction. In A. Liebscher and G. Franz, Eds., *Epidotes*, 56, p. 1–82. *Reviews in Mineralogy and Geochemistry*, Mineralogical Society of America, Chantilly, Virginia.
- Grevel, K.D., Nowlan, E.U., Fasshauer, D.W., and Burchard, M. (2000) In situ X-ray diffraction investigation of lawsonite and zoisite at high pressures and temperatures. *American Mineralogist*, 85, 206–216.
- Hacker, B.R., Abers, G.A., and Peacock, S.M. (2003) Subduction factory: I. Theoretical mineralogy, densities, seismic wave speeds, and H₂O contents. *Journal of Geophysical Research*, 108, 2029 (DOI: 10.1029/2001JB001127).
- Hearmon, R.F.S. (1979) The elastic constants of crystals and other anisotropic materials. *Landolt-Bornstein Tables*, III/11, p. 854. Springer-Verlag, Berlin.
- (1984) The elastic constants of crystals and other anisotropic materials. *Landolt-Bornstein Tables*, III/18, p. 1154. Springer-Verlag, Berlin.
- Holland, T.J.B., Redfern, S.A.T., and Pawley, A.R. (1996) Volume behavior of hydrous minerals at high pressure and temperature: II. Compressibilities of lawsonite, zoisite, clinozoisite, and epidote. *American Mineralogist*, 81, 341–348.
- Hu, J.Z., Mao, H.K., Shu, J., and Hemley, R.J. (1994) High pressure energy dispersive X-ray diffraction technique with synchrotron radiation. In S.C. Schmidt, J.W. Shaner, G.A. Samara, and M. Ross, Eds., *High-Pressure Science and Technology—1993*, 309, p. 441–444. *AIP Conference Proceedings—July 10, 1994*, New York.
- Huang, E. (1999) Raman spectroscopic study of 15 gem minerals. *Journal of the Geological Society of China*, 42, 301–318.
- Jiang, F.M., Speziale, S., Majzlan, J., and Duffy, T.S. (2005) Elastic constants of brucite [Mg(OH)₂] and diaspore [AlO(OH)] to 12 GPa by Brillouin scattering. *EOS, Trans AGU, Fall Meeting Supplement*, MR31A-0119, 2005.
- Laugesen, J.L. (2005) Density functional calculations of elastic properties of portlandite, Ca(OH)₂. *Cement and Concrete Research*, 35, 199–202.
- Nye, J.F. (1985) *Physical Properties of Crystals*, 329 p. Clarendon, Oxford.
- Oda, H., Anderson, O.L., Isaak, D.G., and Suzuki, I. (1992) Measurement of Elastic Properties of Single-Crystal CaO up to 1200 K. *Physics and Chemistry of Minerals*, 19, 96–105.
- Ohno, I., Yamamoto, S., Anderson, O.L., and Noda, J. (1986) Determination of elastic constants of trigonal crystals by the rectangular parallelepiped resonance method. *Journal of Physics and Chemistry of Solids*, 47, 1103–1108.
- O'Neill, B., Bass, J.D., and Rossman, G.R. (1993) Elastic properties of hydrogrossular garnet and implications for water in the upper mantle. *Journal of Geophysical Research*, 98, 20031–20037.
- Pawley, A.R., Chinnery, N.J., and Clark, S.M. (1998) Volume measurements of zoisite at simultaneously elevated pressure and temperature. *American Mineralogist*, 83, 1030–1036.
- Poli, S. and Schmidt, M. W. (1995) Water transport and release in subduction zones: experimental constraints on basaltic and andesitic systems. *Journal of Geophysical Research*, 100, 22299–22314.
- (1998) The high-pressure stability of zoisite and phase relationships of zoisite-bearing assemblages. *Contributions to Mineralogy and Petrology*, 130, 162–175.
- Press, W.H., Flannery, B.P., Teukolsky, S.A., and Vetterling, W.T. (1988) *Numerical Recipes in C: The art of scientific computing*, 735 p. Cambridge University Press, U.K.
- Qin, S., Wu, X., Liu, J., Liu, J., Wu, Z.Y., Li, X.D., and Lu, A.H. (2003) Compressibility of Epidote up to 20 GPa at 298 K. *Chinese Physics Letters*, 20, 1172–1174.
- Ryzhova, T.V., Aleksandrov, K.S., and Korobkova, V.M. (1966) The elastic properties of rock-forming minerals V. Additional data on silicates. *Izvestiya Earth Physics*, 2, 63–65.
- Schilling, F.R., Sinogeikin, S.V., and Bass, J.D. (2003) Single-crystal elastic properties of lawsonite and their variation with temperature. *Physics of the Earth and Planetary Interiors*, 136, 107–118.
- Schmidt, M.W. and Poli, S. (1994) The stability of lawsonite and zoisite at high pressures: Experiments in CASH to 92 kbar and implications for the presence of hydrous phases in subducted lithosphere. *Earth and Planetary Science Letters*, 124, 105–118.
- Shimizu, H. (1995) High-pressure Brillouin scattering of molecular single-crystals grown in a diamond-anvil cell. In M. Senoo, K. Suito, T. Kobayashi, and H. Kubota, Eds., *High Pressure Research on Solids*, p. 1–17. Elsevier, Amsterdam.
- Sinogeikin, S.V., Schilling, F.R., and Bass, J.D. (2000) Single crystal elasticity of lawsonite. *American Mineralogist*, 85, 1834–1837.
- Sondergeld, P., Schranz, W., Troster, A., Carpenter, M.A., Libowitzky, E., and Kityk, A.V. (2000) Optical, elastic and dielectric studies of the phase transitions in lawsonite. *Physical Review B*, 62, 6143–6147.
- Speziale, S. and Duffy, T.S. (2002) Single-crystal elastic constants of fluorite (CaF₂) to 9.3 GPa. *Physics and Chemistry of Minerals*, 29, 465–472.
- Vaughan, M.T. and Weidner, D.J. (1978) The relationship of elasticity and crystal structure in andalusite and sillimanite. *Physics and Chemistry of Minerals*, 3, 133–144.
- Vogel, D.E. and Bahezre, C. (1965) The composition of partially zoned garnet and zoisite from Cabo Ortegal, N. W. Spain. *Neues Jahrbuch für Mineralogie Monatshefte*, 140–149.
- Weidner, D.J. and Carleton, H.R. (1977) Elasticity of coesite. *Journal of Geophysical Research*, 82, 1334–1346.
- Winkler, B., Milman, V., and Nobes, R.H. (2001a) A theoretical investigation of the relative stabilities of Fe-free clinozoisite and orthochoisite. *Physics and Chemistry of Minerals*, 28, 471–474.
- Winkler, B., Hytha, M., Warren, M.C., Milman, V., Gale, J.D., and Schreuer, J. (2001b) Calculation of the elastic constants of the Al₂SiO₅ polymorphs andalusite, sillimanite and kyanite. *Zeitschrift für Kristallographie*, 216, 67–70.

MANUSCRIPT RECEIVED MAY 26, 2006

MANUSCRIPT ACCEPTED OCTOBER 30, 2006

MANUSCRIPT HANDLED BY GUOYIN SHEN